Geodesy and Geodynamics xxx (xxxx) xxx

Contents lists available at ScienceDirect

Geodesy and Geodynamics

journal homepage: http://www.keaipublishing.com/geog

Research Paper

Singular spectrum analysis for the time-variable seasonal signals from GPS in Yunnan Province

WeiJie Tan [a], JunPing Chen [a, b, c, *], YiZe Zhang [a], Bin Wang [a], SongYun Wang [a, c]

[a] Shanghai Astronomical Observatory, Chinese Academy of Sciences, Shanghai 200030, China
[b] School of Astronomy and Space Science, University of Chinese Academy of Sciences, Beijing 100049, China
[c] Shanghai Key Laboratory of Space Navigation and Positioning Techniques, Shanghai 200030, China

ARTICLE INFO

Article history:
Received 21 September 2023
Accepted 6 May 2024

Keywords:
Singular spectrum analysis
Modulated seasonal signals
Time-variable amplitude
GPS draconitic year

ABSTRACT

Studying the seasonal deformation in GPS time series is important to interpreting geophysical contributors and identifying unmodeled and mismodeled seasonal signals. Traditional seasonal signal extraction used the least squares method, which models seasonal deformation as a constant seasonal amplitude and phase. However, the seasonal variations are not constant from year to year, and the seasonal amplitude and phase are time-variable. In order to obtain the time-variable seasonal signal in the GPS station coordinate time series, singular spectrum analysis (SSA) is conducted in this study. We firstly applied the SSA on simulated seasonal signals with different frequencies 1.00 cycle per year (cpy), 1.04 cpy and with time-variable amplitude are superimposed. It was found that SSA can successfully obtain the seasonal variations with different frequencies and with time-variable amplitude superimposed. Then, SSA is carried out on the GPS observations in Yunnan Province. The results show that the time-variable amplitude seasonal signals are ubiquitous in Yunnan Province, and the time-variable amplitude change in 2019 in the region is extracted, which is further explained by the soil moisture mass loading and atmospheric pressure loading. After removing the two loading effects, the SSA obtained modulated seasonal signals which contain the obvious seasonal variations at frequency of 1.046 cpy, it is close with the GPS draconitic year, 1.040 cpy. Hence, the time-variable amplitude changes in 2019 and the seasonal GPS draconitic year in the region could be discriminated successfully by SSA in Yunnan Province.

1. Introduction

The Global Positioning System (GPS) has been widely used to study the Earth's crustal deformation. A way of processing GPS time series for seasonal variations is applying least-squares fitting harmonic terms with a constant amplitude and phase. These methods can ultimately play an indispensable role in exploring the contributions of seasonal sources, such as mass redistributions, thermal expansion, etc [1–5]. However, there are varieties of seasonal crustal processes, such as regional precipitation, local extreme arid climate, are modulated with climate change, i.e., the amplitude and phase of the seasonal signal vary with time [6–14].

The unmodeled seasonal signal, GPS draconitic year with a period of 351.4 days and a frequency of 1.04 circle per year (cpy), can generate beat modulations at 0.04 and 2.04 cpy with the frequency of 1.00 cpy. The two close frequency signals combination can also induce seasonal modulated amplitude variations in GNSS time series [15–22]. Those modulated seasonal variations cannot be measured using the traditional least squares method due to its constant seasonal amplitude and phase assumption.

The advent of Singular spectrum analysis (SSA) provides an appealing opportunity to obtain the time-varying seasonal signals [23–25]. Chen et al. [6] first verified the feasibility of SSA to extract time-varying seasonal signals from GNSS time series. Subsequently, SSA began to be widely used in GNSS data analysis, including the

* Corresponding author. Shanghai Astronomical Observatory, Chinese Academy of Sciences, Shanghai 200030, China.
E-mail address: junping@shao.ac.cn (J. Chen).

Peer review under responsibility of Institute of Seismology, China Earthquake Administration.

Production and Hosting by Elsevier on behalf of KeAi

https://doi.org/10.1016/j.geog.2024.05.002

Please cite this article as: W. Tan, J. Chen, Y. Zhang *et al.*, Singular spectrum analysis for the time-variable seasonal signals from GPS in Yunnan Province, Geodesy and Geodynamics, https://doi.org/10.1016/j.geog.2024.05.002

applications of SSA to extract trend and periodic signals [26–29], effective noise reduction and other purposes [30–33]. Klos et al. [7] further applied different processing methods to extract the modulation amplitude of GNSS time series under different noises, and the results show that SSA can effectively capture seasonal deformation. Guo et al. [10] successfully extracted gravitational solid tides in relative gravity observations based on SSA. Wang et al. [34] applied SSA to obtain seasonal crustal signals, effectively eliminating the influence of noise and local phenomena specific to a single site. Hu et al. [28,29] used SSA to study the GPS seasonal signals caused by hydrological loads in the vertical direction in Yunnan. The results showed that compared with the least squares method, SSA can better reflect the actual seasonal deformation of hydrological loads. Overall, SSA was able to extract the periodic signal of the crust and the seasonal signal with modulated amplitude.

Few studies have demonstrated the ability of SSA to obtain the modulated periodic signals with different frequencies and with time-variable amplitude are superimposed. In this study, we firstly apply singular spectrum analysis on simulated modulated seasonal GNSS time series to demonstrate the abilities of SSA in separating time-variable seasonal signals. Then, we applied the SSA to observed GNSS time series in Yunnan Province and explored the modulated seasonal geophysical process and potential GPS draconitic year.

2. Method and simulation

2.1. Singular spectrum analysis (SSA)

Singular spectrum analysis is a method for time series analysis, which does not require any external assumptions and prior information. Using the basic idea of spatial reconstruction, the original signal components can be identified through singular value decomposition, and the trend, period or quasi-period, and noise in the time series can be realized. Especially for seasonal signals, it is not constrained by the sine wave assumption, and it can stably identify and extract real seasonal signals regardless of the premise that the phase and amplitude are constant [6,7,10,28–31].

The method mainly consists of two stages: matrix factorization and sequence reconstruction. The matrix factorization includes time series embedding and singular value decomposition, and the sequence reconstruction includes grouping and diagonal averaging. Suppose there is a period sequence $Y_N = (y_1, y_2, y_3, \ldots y_N)$, where $N > 2$, assuming with mean subtracted. Take out the equal-length subsequence of Y_N according to the lag-window size L ($1<L < N$), and obtain K ($K=N - L+1$) vectors to form a trajectory matrix by embedding the original sequence, and the trajectory matrix is done in columns [23,35]:

$$X = \begin{bmatrix} y_1 & y_2 & y_3 & \cdots & y_K \\ y_2 & y_3 & y_4 & \cdots & y_{K+1} \\ \vdots & \vdots & \vdots & & \\ y_L & y_{L+1} & y_{L+2} & \cdots & y_N \end{bmatrix} \quad (1)$$

Perform singular value decomposition on the trajectory matrix to obtain L eigenvalues and arrange them in descending order according to the eigenvalues ($\lambda_1 \geq \lambda_2 \geq \lambda_3 \cdots \geq \lambda_L \geq 0$) and the corresponding eigenvectors $U_1, U_2, U_3, \ldots, U_L$. Considering that the first r singular values can reflect the main features of X, a new matrix $Z^{(r)}(r < L)$ is constructed by selecting its eigenvalues and eigenvectors. $\sum_{i=1}^{r}\lambda_i / \sum_{i=1}^{L}\lambda_i$ is the contribution rate of the first r vectors. The purpose of the method is to separate the target component from other signals. Finally, diagonally average the reconstructed component Z to recovery each component of the original time series [23,35]:

$$y = \begin{cases} \dfrac{1}{i}\displaystyle\sum_{j=1}^{i} Z_{j,i-j+1} & 1 \leq i \leq L-1 \\ \dfrac{1}{L}\displaystyle\sum_{j=1}^{L} Z_{j,i-j+1} & L \leq i \leq K \\ \dfrac{1}{N-i+1}\displaystyle\sum_{j=i-K+1}^{N-K+1} Z_{j,i-j+1} & K+1 \leq i \leq N \end{cases} \quad (2)$$

where the signal y recovered by SSA is obtained, that is, the extraction and separation of the signal is realized.

According to the SSA, when there is periodic component in the original sequence, SSA will obtain a pair of recovered components whose eigenvalues are nearly equal, and their corresponding eigenvectors are orthogonal respectively. A periodic component of the original sequence is the sum of a pair of recovered components that satisfy these conditions. Details of the supplementary can be found in previous studies [6,23,25], which will not be described in this paper.

2.2. Simulation test

The modulated seasonal signals are usually caused by the geophysical processes or similar frequency singles, which are both involved in the test. In order to verify the feasibility of SSA in obtaining similar frequency signals, the station coordinate time series of 10 years and 3653 epochs in a single day were simulated. The simulated data included the two different periodic signals of 1.00 cpy and 1.04 cpy, as well as the modulation amplitude. The simulated signals are expressed as follows:

$$\begin{aligned} S(t_i) = {} & a\sin(2\pi t_i) + b\cos(2\pi t_i) + c(t_i)\sin(2\pi t_i) \\ & + c(t_i)\cos(2\pi t_i) + d\sin(1.04\times 2\pi t_i) \\ & + e\cos(1.04\times 2\pi t_i) + \varepsilon(t_i) \end{aligned} \quad (3)$$

where, t_i is the decimal point year; a, b are the stable constant amplitudes with a frequency of 1.00 cpy. Since the global mean annual amplitude is about 4 mm [1], we set the $a = 4$, $b = 1$ in our simulation. d, e are the stable amplitudes with a frequency of 1.04 cpy. For the GPS draconitic year in the GNSS time series, we know little about its variation in the time domain, especially the seasonal amplitude. GPS draconitic year is usually a hidden time series residual. Thus, we set the $d = 2$, $e = 1$ in our simulation. $c(t_i)$ is the modulation amplitude of a signal at frequency 1.00 cpy, the mathematical expression is as follows [6]:

$$c(t_i) = e^{0.5\,\sin(t_i)} \quad (4)$$

Considering that the GPS station coordinates time series often contains noise information [36,37], we adopt a flicker noise model $\varepsilon(t_i)$ in simulated time series following the previous study [37]. The simulated data are shown in Fig. 1a and b.

Using SSA to carry out signal extraction, the lag-window of this decomposition is 365 days (see Section 2.3 for the selection of the lag-window), and the extracted modulated amplitude seasonal signal by SSA is shown in Fig. 1b, black line. The eigenvalues are represented by the proportion of the data variance (Fig. 2), which represent the contributor to the original time series, usually related to the main source time function. The eigenvalue results show that the first and second components account for 33.91% and 32.99%, respectively, and the other components account for much less than

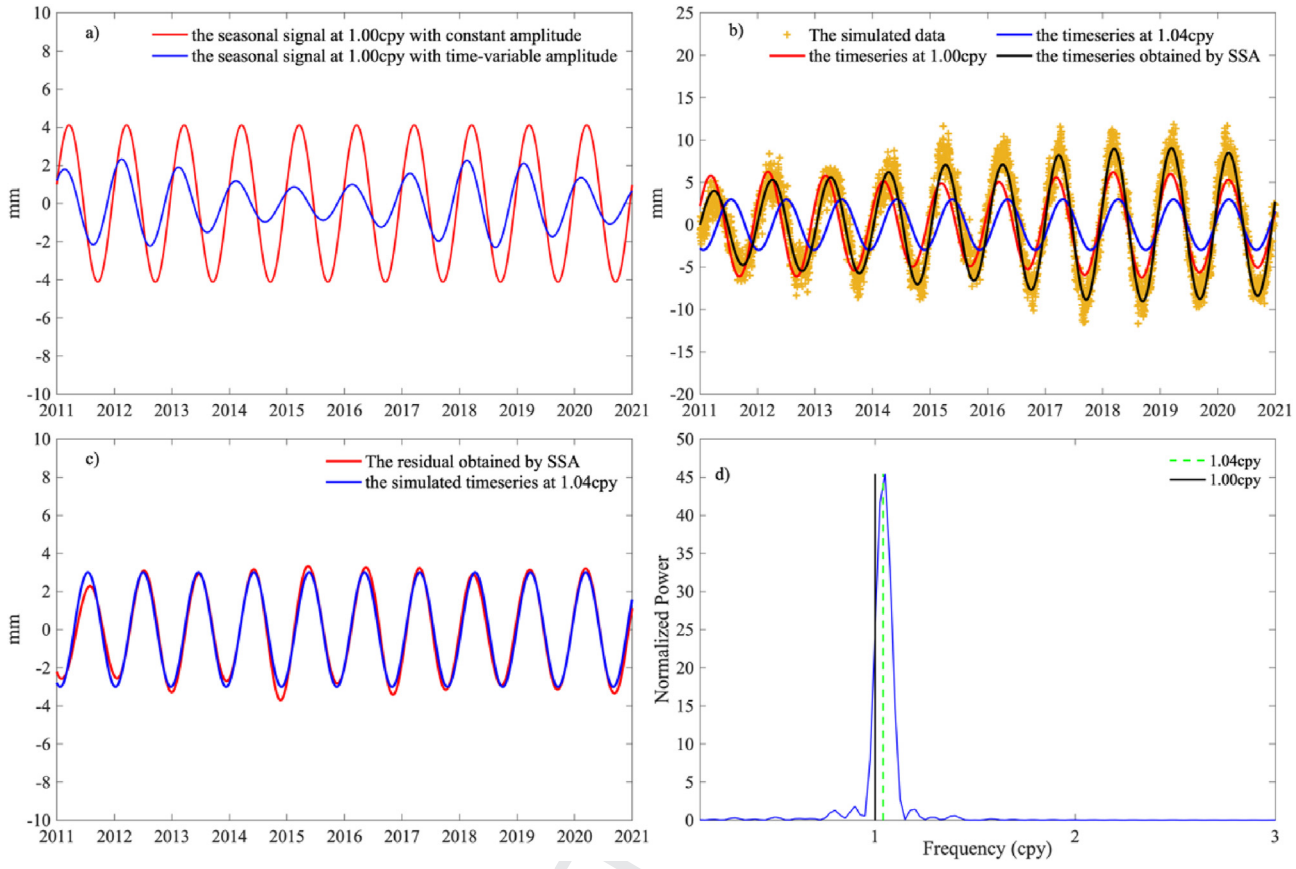

Fig. 1. Singular spectrum analysis for amplitude-modulated seasonal signals in simulated data. a) The simulated time series of constant amplitude and time-variable amplitude with a frequency of 1.00 cpy; b) The time series obtained in a) with a frequency of 1.00 cpy (red line) and the simulated time series with a frequency of 1.04 cpy (blue line), the combined time series with 1.00 cpy and 1.04 cpy, which also considering the flicker noise (yellow scatter), and the black line is the seasonal signal recovered by SSA; c) SSA residual (red line, the recovered signal of SSA with the removement of the time series at 1.00 cpy) and the simulated time series of 1.04 cpy (blue line); d) The spectrum analysis of SSA residual. The black vertical solid line indicates seasonal signals (1.0 cpy), and the green dashed line indicates anomalous harmonics at 1.04 cpy.

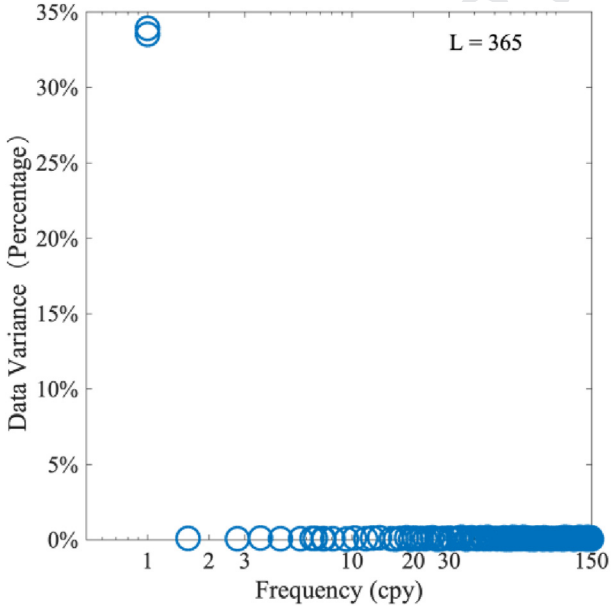

Fig. 2. Eigenvalues versus the dominant frequency associated with their corresponding eigenvectors.

2%, indicating that the first two components contain the main information of the original data. The first two eigenvalues are nearly equal, which means the sum of the two components contain the main periodic component in the original sequence [6,23,25]. The spectral analysis of the components extracted by SSA shows that the first two components have obvious periodicity, and the peaks of the periodic spectrum are at 1.00 cpy and 1.025 cpy, respectively, while the other components do not. Therefore, the first two components are applied for data recovery. The results show that with a lag-window of 365 days, the variance of the data obtained by SSA is 66.90% (Table 1), and the true proportion of the variance for the periodic signal in the simulated signal is 67.16%. Therefore, SSA can recover 99.61% of the original data in the simulation test.

The SSA-recovered signal was further processed: the simulated annual signal was subtracted from the SSA-recovered signal to obtain the residual (called the SSA residual) (Fig. 1c, red line). The RMS (Root Mean Square) between the SSA residual and the simulated GPS draconitic year is 0.23 mm. Spectral analysis revealed (Fig. 1d) that SSA residuals had a significant frequency at 1.050 cpy, slightly different from the simulated GPS draconitic year (1.04 cpy). The frequency difference between SSA residual and theoretical values may be due to the length of time in the data [15,19,21,22] as well as noise in the time series. The results show that SSA can extract the modulated amplitude signal with different frequencies and with

time-variable amplitude superimposed in the simulated time series, and the recovered seasonal signal by SSA contains the coupled signals of close frequencies, and finally, the separation of similar frequency signals can be achieved through further processing.

2.3. Selection of lag-window length

In the SSA method, the lag-window L and component selection for data recovery are crucial. If the window is too large, the recovered signals will alias; if the window is too small, the signals cannot be completely separated. Since the singular value decomposition of the trajectory matrix for window lengths L and K is symmetric, it is not necessary for the window length L to exceed $N/2$ [25]. Vautard et al. [23] demonstrated that SSA can obtain the periodic signal between $L/5$ and L. For geodetic applications, Rangelova et al. [24] applied a 3-year window, which is half of the data length ($N/2$), to obtain the signals. Chen et al., 2013 demonstrated that a window size of 2 or 3 years (less than $N/4$) can be appropriate to obtain the annual and semi-annual signals from GPS time series. In addition, Khan and Poskitt [38] also propose a mathematical method of window length selection. As we are interested in the close frequency extraction around the annual variations, we follow the previously demonstrated results and perform different window length tests in this work.

Considering the GPS time series are single-day observations, and we mainly focus on the annual seasonal signal, the lag-window of 90 days, 182 days (1/2 year), 365 days (1 year), and 730 days (2 years) are selected.

When a smaller lag-window of 90 days was selected, the recovered SSA residual frequency was 1.025 cpy (Table 1), a significant deviation from the theoretical value. When the lag-window was selected as 182 days, 365 days, or 730 days, the frequency of the obtained SSA residual is 1.050 cpy, close to the theoretical value of 1.040 cpy. On the one hand, because the data length is 10 years, less than 25 years, there may be deviations in separating these two similar frequency signals. In addition, there is obvious noise in the simulated data, which may cause frequency deviation. The RMS of the difference between the theoretical value and the SSA residual shows that the larger window guarantees the recovery of the seasonal signal to the original data (Table 1). However, the larger window may split part of the main variance into other artificial long-term variations [6]. Thus, we apply the data variance to recovery from the desired signal (Table 1). The recovery variance results show that the larger window did deviate from the recovery of the desired signal. Therefore, the tests show that 182 days and 365 days are appropriate window choices. We apply 365 days as the embedded data lag-window for further work in this study.

3. GNSS data analysis

3.1. GNSS station coordinate data and research area

We used the GNSS observations from 2011 to 2021 (Fig. 3) of 25 GNSS stations built by the Crustal Movement Observation Network of China (CMONOC) in Yunnan Province. The data comes from the GNSS Analysis Center of Shanghai Astronomical Observatory, Chinese Academy of Sciences (SHA, http://www.shao.ac.cn/shao_gnss_ac). The Shanghai Astronomical Observatory uses the high-precision geodetic analysis system iGPOS software to process GPS observation data. The estimated parameters include station coordinates and tropospheric parameters, satellite orbits, and earth orientation parameters. The calculated station coordinates are transformed into the framework of ITRF2008 through Helmert transformation. The results provided by the analysis center are consistent with the accuracy of IGS products. The horizontal accuracy of station coordinates is 3 mm, and the vertical accuracy is 6 mm. For detailed processing methods of GNSS data, see Chen et al. [39].

The GPS time series post-processing applied the known models and uses the least square method to estimate station trend items, annual and semi-annual items, and jumps caused by seismic activity or instrument replacements. Fig. 3 shows the residuals after processing using the least squares method. In Fig. 3, a significant non-linear variation is observed around 2019 in the station coordinate residual time series obtained by using the traditional least squares fitting method. At the same time, the article by Tan et al. (2022) pointed out that the station coordinate time series in Yunnan Province also contains a periodic signal of 1.04 cpy. In this work, we apply SSA to extract the modulated seasonal signal in the region. Here, we mainly focus on the seasonal signal in the time series, so we retain the annual signal information for data processing in the residual series.

3.2. The modulated seasonal signals in GPS extracted by SSA

We apply SSA to the GPS seasonal residuals which contain seasonal deformation signals. According to the selection of the lag-window in 2.3, the SSA is performed on a lag-window of 365 days to obtain the seasonal deformation of each station. Since we mainly focus on seasonal signals, whether the recovered signal contains obvious periodic changes is a crucial impactor. SSA was performed on the time series of 25 GNSS stations to obtain the seasonal signals of each station. Finally, we choose the reconstructed components of the first two singular spectral components (The mean data variance contribution is about 41%), which both show obvious periodic changes. Then, the 25 seasonal signals recovered by SSA in Yunnan Province were further processed using the stacking method (Fig. 4a, red line). Sometimes, data gaps exist in the GPS time series, we fill time gaps with linear interpolation. At the same time, the traditional least-squares fitting (lsq) harmonic terms with a constant amplitude and phase were used to fit the annual signal in the region. The stacking method is also applied on the seasonal signal obtained by lsq (Fig. 4a, yellow line).

Compared with the annual deformation obtained by the traditional method lsq, the modulated-amplitude seasonal signal in the Yunnan region obtained by SSA changes significantly over time (Fig. 4a, red line). Its amplitude was slightly smaller than the constant amplitude annual signal fitted by the least square method in 2014 and 2017, and was significantly larger than the constant amplitude annual signal around 2019. The phases of the seasonal

Table 1
The data variance, frequency of recovered seasonal signals with different lag-window. The RMS between the SSA residual and the theoretical signals.

	The real data variance	lag-window L (days)			
		90	182	365	730
The simulated data	67.16%				
The recovery variance		67.53%	67.00%	66.90%	66.87%
SSA residual frequency (cpy)		1.025	1.050	1.050	1.050
the difference between the theoretical value and the SSA residual RMS (mm)		0.46	0.35	0.23	0.20

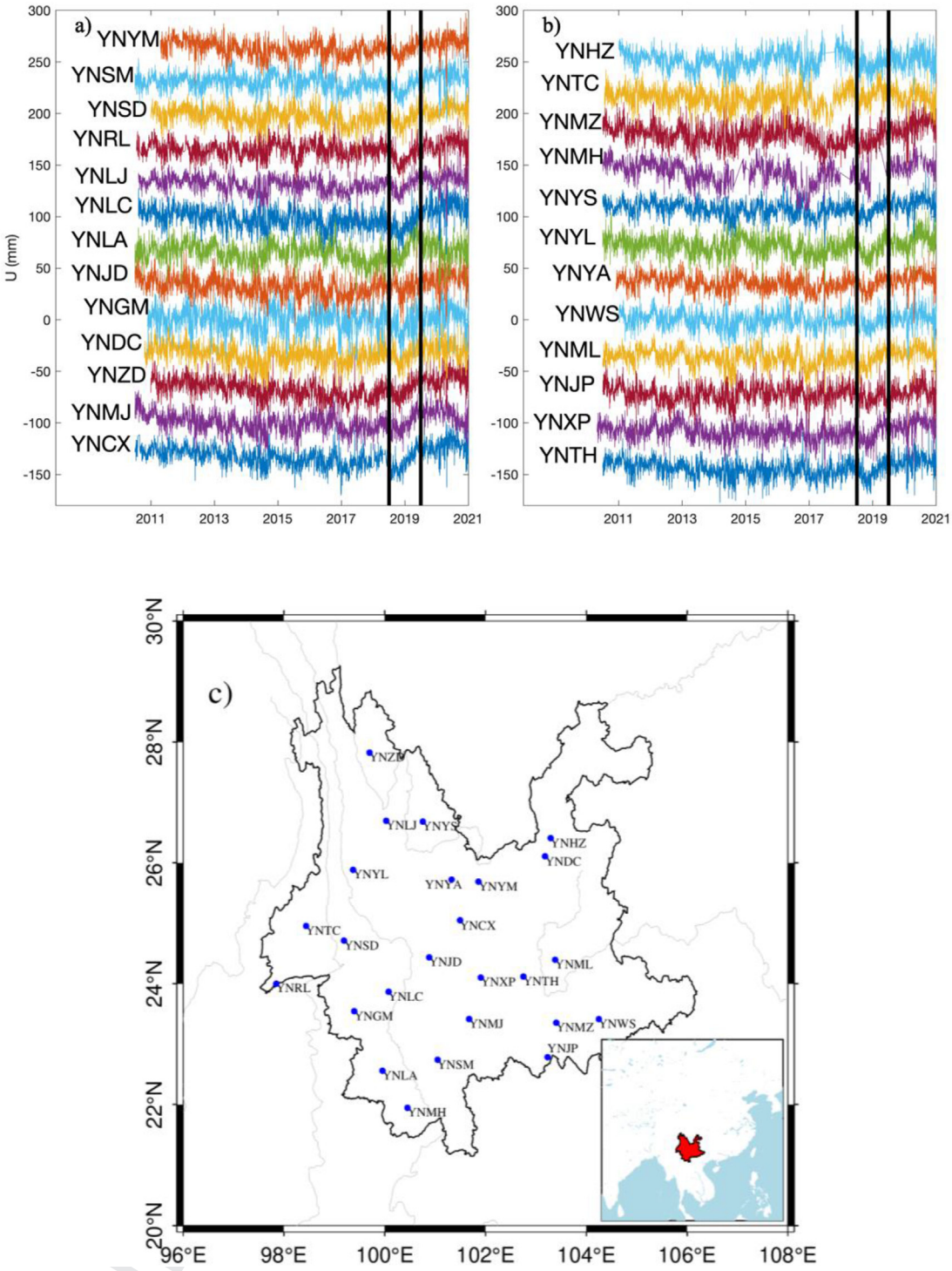

Fig. 3. a) and b) The GPS residuals (the linear term, seasonal terms and obvious jumps are removed) in Yunnan Province. c) The GPS sites' location map.

signals obtained by the two methods are consistent in visual. Since we mainly concentrate on the modulated seasonal amplitude variations, we leave a detailed discussion about the phase variations for further study. The difference in amplitude and the basic coincidence of phase indicates that the seasonal deformation in this region is mainly caused by the mass redistributions [1]. We will discuss the geophysical contributors to the modulated seasonal signals in the latter Section 4.1.

The residual RMS obtained by SSA is 5.0 mm; the residual obtained by the least square method is 5.9 mm. Thus, SSA can improve the GPS data analysis accuracy to a certain extent. This phenomenon can be seen more intuitively by subtracting the least-squares fitted steady-state annual signal from the seasonal signal recovered from SSA (Fig. 4b, yellow line). As discussed before, the modulated seasonal signals usually contain the time-varying mass loading variations or the error of the GPS system (GPS draconitic

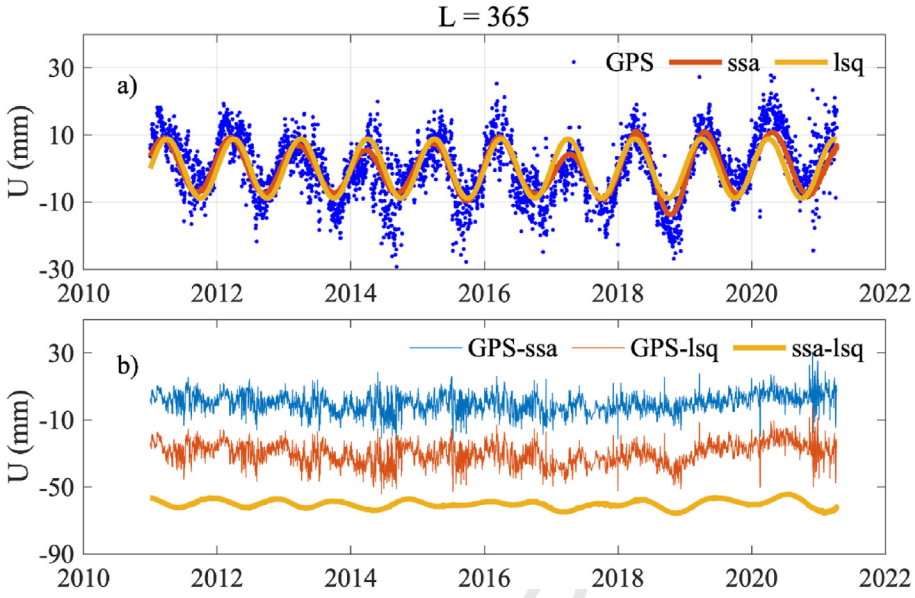

Fig. 4. a) The seasonal signals in Yunnan Province obtained by SSA and lsq from the GPS seasonal residuals. b) The residual with SSA (GPS − ssa) and lsq (GPS − lsq, the time series is offset −30 mm to avoid overlap of symbols), and the different of the two residuals (ssa − lsq, the time series is offset −60 mm to avoid overlap of symbols).

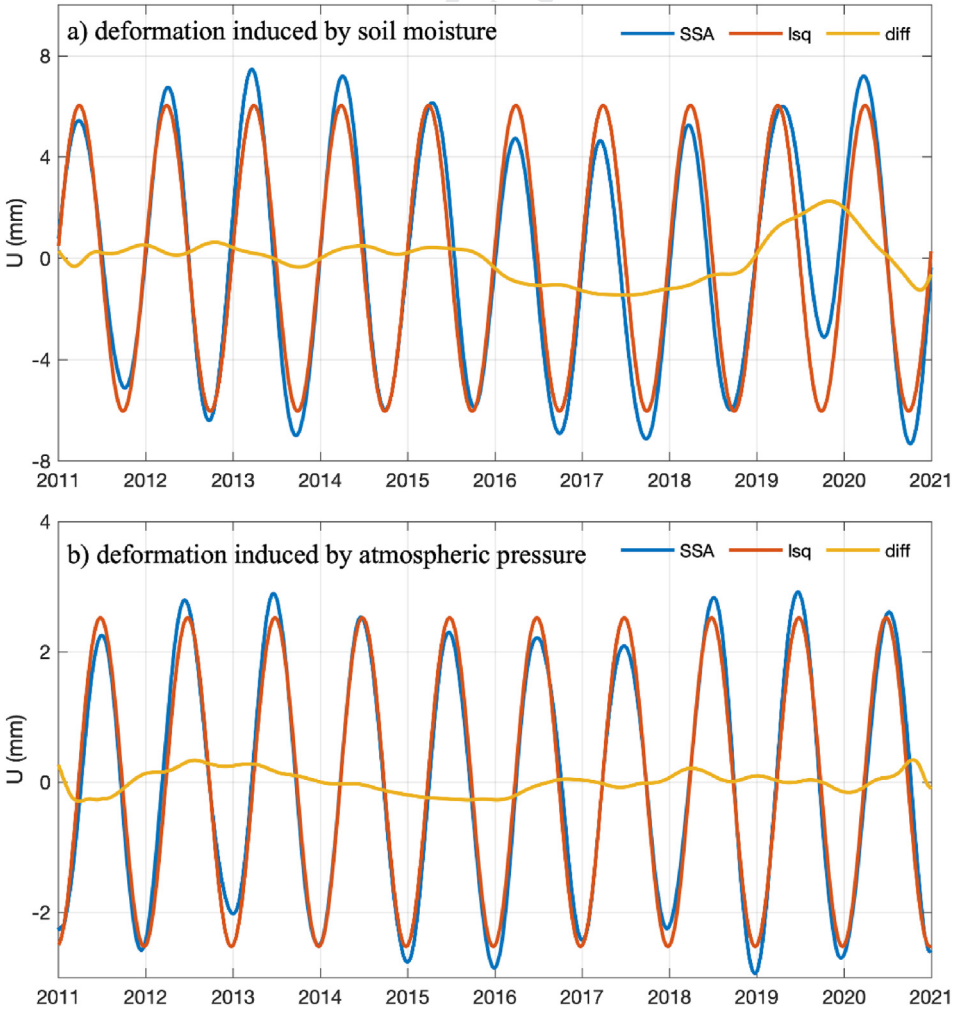

Fig. 5. The seasonal deformation of the soil moisture and atmospheric pressure obtained by SSA and lsq, and the difference between the two methods (diff, yellow lines).

year). We then make discussion in the following sections about the two aspects.

4. The sources to the modulated seasonal signals

4.1. The geophysical contributors to modulated seasonal signals

Surface atmospheric pressure, hydrologic cycle, and non-tidal ocean loading are the main source factors affecting vertical seasonal displacements observed by GPS [1,8]. At the same time, the amplitude of those mass redistributions changes over time, especially for the displacement caused by water storage [5,12,13]. The soil moisture and atmospheric pressure are the main factors affecting the surface load deformation in Yunnan Province; the snow variation and non-tidal ocean loading induced deformation are less than 0.5 mm in the region [28,29,40,41]. Thus, we only calculate the surface deformation caused by the atmospheric pressure and soil moisture mass loadings in this work.

The atmospheric surface pressure data provided by NCEP (National Centers for Environmental Prediction) (http://www.esrl.noaa.gov) was used to calculate the surface deformation caused by atmospheric loading. The spatial resolution of the model is 2.5° × 2.5°, and the temporal resolution is 6 h. The NCEP Reanalysis II single-day soil water model was used to calculate deformation caused by soil moisture mass loading in Yunnan Province, with a spatial resolution of 1.875° × 1.875°. We calculate the ground deformation by Green's function method [42] and the models data span from 2011 to 2021 We firstly calculate the crustal deformation of each station with a time resolution of one day, and then we use the same fitting method as the GPS time series to obtain the seasonal surface deformation caused by the two above geophysical phenomena by using the SSA and lsq, respectively (Fig. 5).

As shown in Fig. 5, the amplitude of the seasonal deformation caused by soil moisture loading and atmospheric loading varies significantly with time. Comparing the difference of seasonal signals obtained by the SSA and lsq (Fig. 5, diff , yellow line), it is found that the crustal deformation caused by soil moisture has an obvious modulation amplitude change process around 2019. For the atmospheric loading induced deformation, no significant changes were observed in the time. Considering the influence of the two mass loadings on the station coordinates, we deduct the atmospheric load and soil moisture induced deformation from GPS observations, and compare the effects before and after the deducting of the two mass loads (Fig. 6). In order to highlight the non-linear variations around 2019, a sliding window of 365 days is applied on the residuals. It is found that after deducting the deformation caused by the atmospheric pressure and soil moisture, the residuals of the GPS station coordinate time series do not have obvious non-linear variation around 2019, which verifies that the seasonal amplitude of the GPS over time in 2019 is due to the mass redistributions.

We also consider the heavy precipitation or extreme climate in Yunnan Province around 2019. Based on this, we obtain the monthly average precipitation data provided by the National Meteorological Science Data Center (http://data.cma.cn/), and its time span, from 2011 to 2021, is consistent with the GPS observations. By deducting the average precipitation of each month in the 10 years, the precipitation anomaly data in Yunnan Province from 2011 to 2021 were obtained (Fig. 7). In order to highlight the non-linear variations of the precipitation, a sliding window of 12

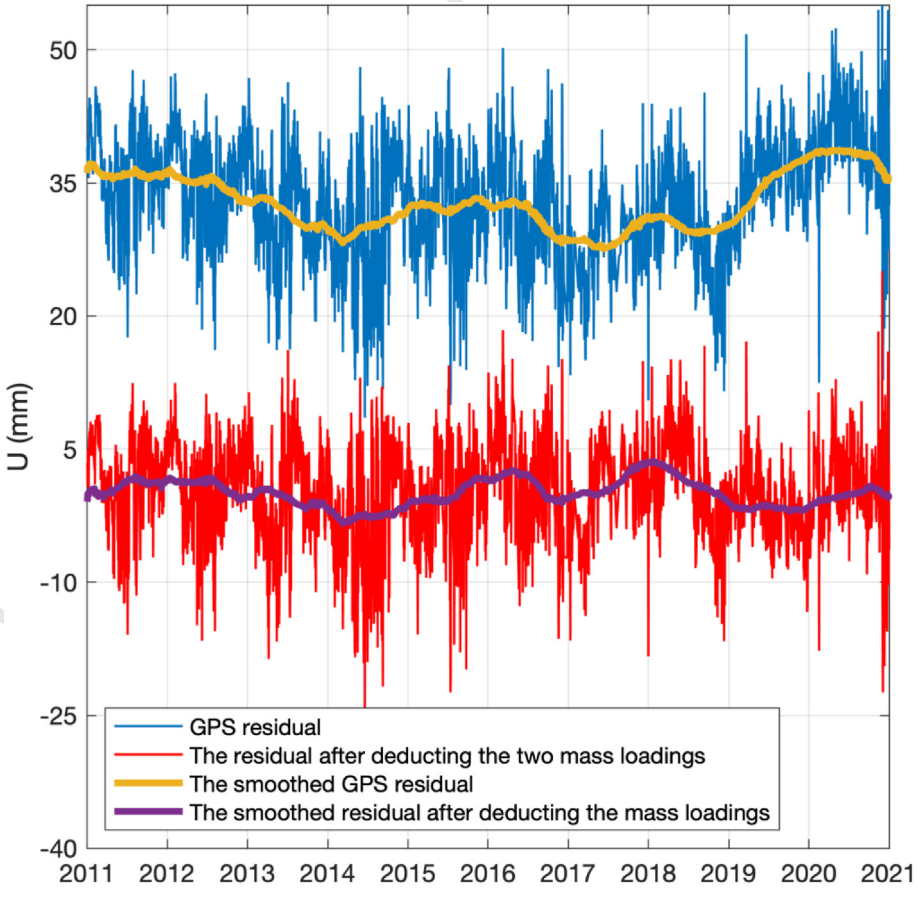

Fig. 6. The GPS residual before and after removing the atmospheric load and soil moisture.

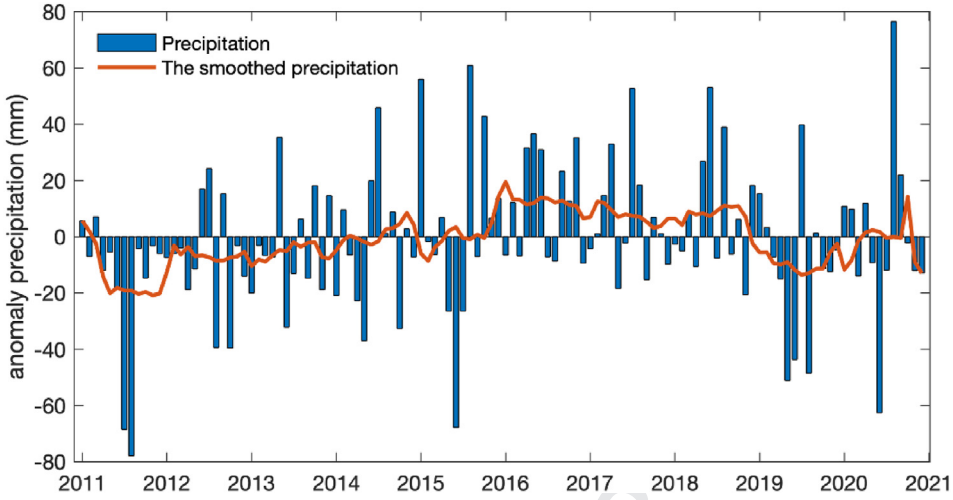

Fig. 7. The anomaly precipitation and the smoothed anomaly precipitation from 2011 to 2021 in Yunnan Province.

months also applied on precipitation anomaly (Fig. 7, red line). There was obviously heavy precipitation in Yunnan Province in 2019. At the same time, the region also had obvious heavy precipitation anomaly in 2011 (Fig. 7), but no abnormal deformation signal was observed in the GPS station coordinate time series (Fig. 6). This is because precipitation is only a part of the hydrological cycle, which continually exchanges through surface runoff, ground evaporation, transpiration, and terrestrial water storage. The current results show that precipitation is not directly related to anomalous crustal non-linear variations in 2019 observed by GPS.

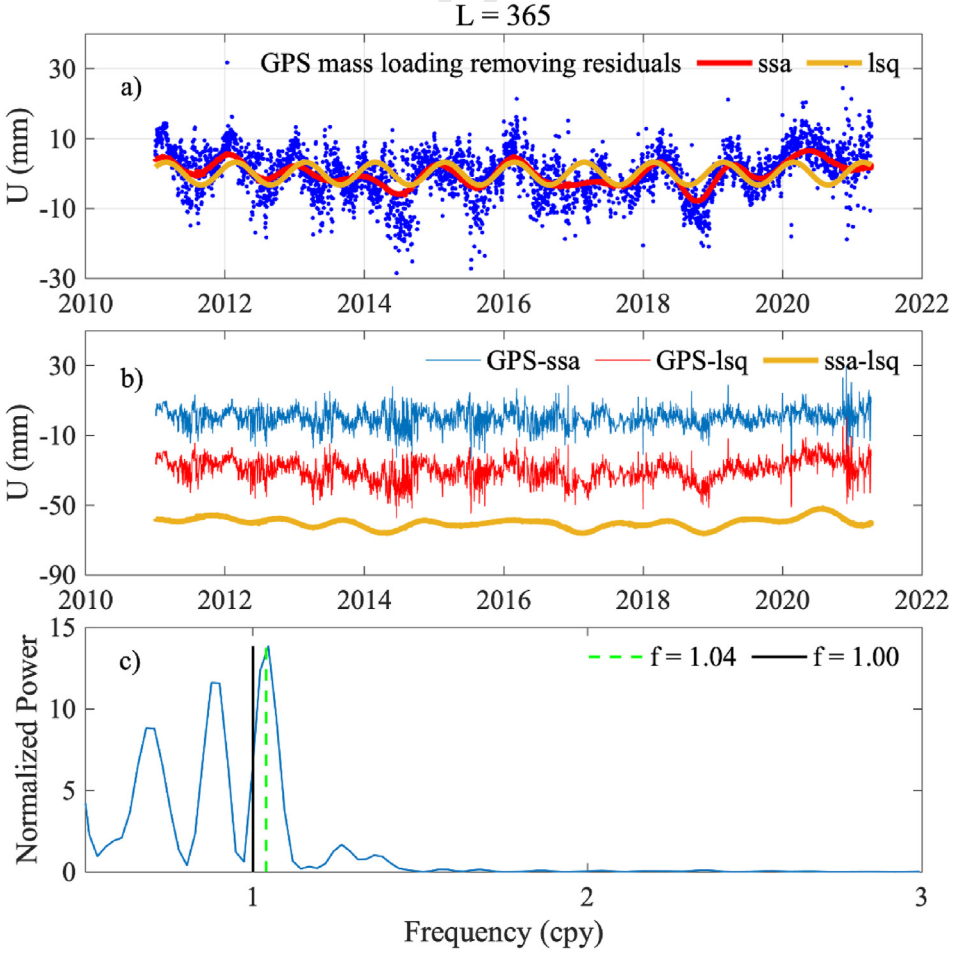

Fig. 8. a) The GPS residual after removing the mass loadings and the seasonal time series obtained by SSA and lsq. b) The residual with SSA (GPS − ssa) and lsq (GPS − lsq, the time series is offset −30 mm to avoid overlap of symbols), and the different of the two residuals (ssa − lsq, the time series is offset −60 mm to avoid overlap of symbols). c) The spectrum analysis of difference between SSA residuals and lsq residual.

The detailed discussion of the interaction between precipitation and other hydrological cycle processes needs further study.

4.2. The error source to the modulated seasonal signals

We have demonstrated that the atmospheric pressure and soil moisture mass loadings are the main contributors to the modulated seasonal source 2019 of the GPS time series. As we discussed above, the combination of GPS draconitic year and annual variations can also cause time-varying seasonal variations. Thus, we deduct the atmospheric pressure and soil moisture mass loadings deformation from GPS observations to obtain GPS mass loading removing residuals (Fig. 8a, blue scatter). According to the previous data processing method, the seasonal signal is extracted using SSA (Fig. 8a, red line) and least square method (Fig. 8a, yellow line), respectively. Comparing the results of the two methods, obvious amplitude differences are seen visually. Then we obtain the difference time series of the two methods (Fig. 8b, yellow lines) and perform frequency analysis. The frequency analysis shows that the difference time series is at frequency of 1.046 cpy, which is close to the GPS draconitic year frequency compared with the previous studies [15,16,22]. Based on the results, it is considered that the periodic mass loading deformation and GPS draconitic year are both included in the modulation seasonal deformation obtained by SSA.

5. Conclusion

The seasonal variations in GPS time series include the crustal annual deformation, the GPS draconitic year, other unknown crustal deformation signals and noise, etc. Simulation tests show that the seasonal signal extracted by SSA contains seasonal variations with close frequencies of 1.04 cpy and 1.00 cpy, and with modeled time-variable amplitude seasonal signals. Applying SSA to the observed GNSS time series in Yunnan Province, the main results include: 1) There is a modulated seasonal amplitude in the GPS station coordinates time series in the region; 2) The obtained modulation amplitude in 2019 is related to the load deformation caused by soil moisture loading and atmospheric pressure loading. 3) After deducting the mass loading effects, SSA has obtained the seasonal variations close to the frequency of the GPS draconitic year of 1.04 cpy. In conclusion, the SSA obtained the modulated seasonal signals containing the time-variable amplitude of seasonal mass loading variations and time-variable amplitude induced by close frequencies of the GPS draconitic year at 1.04 cpy and annual signals at 1.00 cpy. However, the processing method in the paper is to subtract the annual signal with constant periodic amplitude from the seasonal signal obtained by SSA, which may cause processing errors; and SSA cannot directly extract periodic signals with similar frequencies of 1.00 cpy and 1.04 cpy, which means similar frequency signals extraction by SSA needs further study.

Author statement

The authors declare that there is no other statements.

Declaration of competing interest

Q3 The authors declare that there is no conflicts of interest.

Acknowledgments

Q4 This research was funded by National Natural Science Foundation of China (Grant No. 11803065), Natural Science Foundation of Shanghai (Grant No. 22ZR1472800).

References

[1] D. Dong, P. Fang, Y. Bock, et al., Anatomy of apparent seasonal variations from GPS-derived site position time series, J. Geophys. Res. Solid Earth 107 (B4) (2002). ETG 9-1-ETG 9-16.
[2] M. Wang, Z. Shen, D. Dong, Effects of non-tectonic crustal deformation on continuous GPS position time series and correction to them, Chin. J. Geophys. 48 (5) (2005) 1045–1052.
[3] J.L. Davis, B.P. Wernicke, M.E. Tamisiea, On seasonal signals in geodetic time series, J. Geophys. Res. Solid Earth 117 (B1) (2012).
[4] D. Dong, J. Chen, J. Wang, GNSS high-precision position, China Science Publishing & Media Ltd., 2018.
[5] W. Jiang, K. Wang, Z. Li, et al., Prospect and theory of GNSS coordinate time series analysis, Geomatics Inf. Sci. Wuhan Univ. 43 (12) (2018) 2112–2123.
[6] Q. Chen, T. van Dam, N. Sneeuw, et al., Singular spectrum analysis for modeling seasonal signals from GPS time series, J. Geodyn. 72 (2013) 25–35.
[7] A. Klos, M.S. Bos, J. Bogusz, Detecting time-varying seasonal signal in GPS position time series with different noise levels, GPS Solut. 22 (1) (2018).
[8] W. Jiang, P. Yuan, H. Chen, et al., Annual variations of monsoon and drought detected by GPS: a case study in Yunnan, China, Sci. Rep. 7 (2017) 1–10.
[9] Z. Jiang, Y.J. Hsu, L. Yuan, et al., Monitoring time-varying terrestrial water storage changes using daily GNSS measurements in Yunnan, southwest China, Rem. Sens. Environ. 254 (April 2020) (2021) 112249.
[10] J. Guo, W. Gao, H. Yu, et al., Gravity tides extracted from relative gravimetric data with singular spectrum analysis, Chin. J. Geophys. 61 (10) (2018) 3889–3902.
[11] G. Su, W. Zhan, Abnormal depletion of terrestrial water storage and crustal uplift owing to the 2019 drought in Yunnan, China, Geophys. J. Int. 231 (1) (2022) 108–117.
[12] M. Tang, P. Zhong, Z. Jiang, et al., Investigation of spatiotemporal characteristics of terrestrial water storage changes in the Yangtze River Basin using GNSS vertical displacement data, Chin. J. Geophys. 65 (10) (2022) 3780–3796.
[13] X. Yang, L. Yuan, Z. Jiang, et al., Quantitative analysis of abnormal drought in Yunnan Province from 2011 to 2020 using GPS vertical displacement observations, Chin. J. Geophys. 65 (8) (2022) 2828–2843.
[14] Y. Jia, X. Zhu, F. Sun, et al., Time-varying characteristics and cause analysis of annual amplitudes of GNSS vertical coordinate time series, Chin. J. Geophys. 66 (1) (2023) 162–172.
[15] J. Ray, Z. Altamimi, X. Collilieux, et al., Anomalous harmonics in the spectra of GPS position estimates, GPS Solut. 12 (1) (2008) 55–64.
[16] J. Ray, J. Griffiths, X. Collilieux, et al., Subseasonal GNSS positioning errors, Geophys. Res. Lett. 40 (22) (2013) 5854–5860.
[17] A.R. Amiri-Simkooei, On the nature of GPS draconitic year periodic pattern in multivariate position time series, J. Geophys. Res. Solid Earth 118 (5) (2013) 2500–2511.
[18] J. Bogusz, A. Klos, On the significance of periodic signals in noise analysis of GPS station coordinates time series, GPS Solut. 20 (2016) 655–664.
[19] M. Li, S. Guo, N. Wei, et al., Study on the draconitic year errors in GPS station coordinates, Prog. Geophys. 33 (2) (2018) 473–478.
[20] R. Zajdel, K. Sośnica, G. Bury, et al., System-specific systematic errors in earth rotation parameters derived from GPS, GLONASS, and Galileo, GPS Solut. 24 (3) (2020).
[21] S. Guo, C. Shi, N. Wei, et al., Effect of ambiguity resolution on the draconitic errors in sub-daily GPS position estimates, GPS Solut. 25 (3) (2021) 1–14.
[22] W. Tan, D. Dong, J. Chen, Application of independent component analysis to GPS position time series in Yunnan Province, southwest of China, Adv. Space Res. 69 (11) (2022) 4111–4122.
[23] R. Vautard, P. Yiou, M. Ghil, Singular-spectrum analysis: a toolkit for short, noisy chaotic signals, Phys. Nonlinear Phenom. 58 (1–4) (1992) 95–126.
[24] E. Rangelova, M.G. Sideris, J.W. Kim, On the capabilities of the multi-channel singular spectrum method for extracting the main periodic and non-periodic variability from weekly GRACE data, J. Geodyn. 54 (2012) 64–78.
[25] N. Golyandina, Particularities and commonalities of singular spectrum analysis as a method of time series analysis and signal processing, Wiley Interdisciplinary Reviews: Comput. Stat. 12 (4) (2020) e1487.
[26] Y. Shen, F. Peng, B. Li, Improved singular spectrum analysis for time series with missing data, Nonlinear Process Geophys. 22 (4) (2015) 371–376.
[27] A. Klos, M. Gruszczynska, M.S. Bos, et al., Estimates of vertical velocity errors for IGS ITRF2014 stations by applying the improved singular spectrum analysis method and environmental loading models, Geodynamics and Earth tides observations from global to micro scale (2019) 229–246.
[28] S. Hu, T. Wang, Y. Guan, et al., Analyzing the seasonal fluctuation and vertical deformation in Yunnan province based on GPS measurement and hydrological loading model, Chin. J. Geophys. 64 (8) (2021) 2613–2630.
[29] S. Hu, T. Wang, Y. Guan, et al., Yunnan region vertical GPS time series periodic signal extraction based on SSA, Sci. Surv. Mapp. 46 (8) (2021) 33–40.
[30] C. Lu, C. Kuang, Z. Yi, et al., Singular spectrum analysis Filter method for mitigation of GPS multipath error, Geomatics Inf. Sci. Wuhan Univ. 40 (7) (2015) 924–931.
[31] Y. Luo, C. Kuang, C. Lu, et al., GPS coordinate series denoising and seasonal singnal extraction based on SSA, J. Geodesy Geodyn. 35 (3) (2015).
[32] H. Dai, A. Xu, W. Sun, Signal denoising method based on improve singular spectrum analysis, Trans. Beijing Inst. Technol. 36 (7) (2016) 727–732. ,759.

[33] M. Zhou, J. Guo, Y. Shen, et al., Extraction of common mode errors of GNSS coordinate time series based on multi-channel singular spectrum analysis, Chin. J. Geophys. 61 (11) (2018) 4383–4395.
[34] H. Wang, J. Yue, Y. Xiang, et al., Seasonal signal extraction of regional GPS stations based on MSSA, J. Geodesy Geodyn. 39 (5) (2019).
[35] R. Vautard, M. Ghil, Singular spectrum analysis in nonlinear dynamics, with applications to paleoclimatic time series, Phys. D: Nonlinear Phenom. 35 (1989) 395–424.
[36] S. Williams, Error analysis of continuous GPS position time series, J. Geophys. Res. 109 (B3) (2004) 1–19.
[37] W. Wang, X. Qiao, D. Wang, et al., Spatiotemporal noise in GPS position time-series from crustal movement observation Network of China, Geophys. J. Int. 216 (3) (2019).
[38] M.A.R. Khan, D.S. Poskitt, Moment tests for window length selection in singular spectrum analysis of short–and long–memory processes, J. Time Anal. 34 (2) (2013) 141–155.
[39] J. Chen, B. Wu, X. Hu, et al., SHA: the GNSS analysis center at SHAO, in: China satellite navigation conference (CSNC) 2012 proceedings, Springer, Berlin, Heidelberg, 2012, pp. 213–221.
[40] C.Z. Sheng, W.J. Gan, S.M. Liang, et al., Identification and elimination of non-tectonic crustal deformation caused by land water from GPS time series in the western Yunnan province based on GRACE observations, Chin. J. Geophys. 57 (1) (2014) 42–52.
[41] W. Tan, J. Chen, D. Dong, et al., Analysis of the potential contributors to。common mode error in Chuandian region of China, Rem. Sens. 12 (5) (2020) 751.
[42] W.E. Farrell, Deformation of the Earth by surface loads, Rev. Geophys. 10 (1972) 761–797.

Weijie Tan is currently an associate research scientist at Shanghai Astronomical Observatory (SHAO), Chinese Academy of Sciences (CAS). She received her Ph.D. degree from Shanghai Astronomical Observatory (SHAO), Chinese Academy of Sciences (CAS) in 2017. She is mainly engaged in the research of GNSS data processing and coordinate time series。

Junping Chen is a professor and the head of the GNSS data analysis group at Shanghai Astronomical Observatory (SHAO), Chinese Academy of Sciences (CAS). He received his Ph.D. degree in Satellite Geodesy from Tongji University in 2007. He worked as a research scientist at the GFZ German Research Centre for Geosciences from 2006 to 2011. Since 2011, he has been supported by the "one hundred talents" program of the Chinese Academy of Sciences. His research interests include multi- GNSS data analysis and GNSS augmentation systems.

Yize Zhang is currently an associate professor at Shanghai Astronomical Observatory (SHAO), Chinese Academy of Sciences (CAS). He received his Ph.D. degree from Tongji University in 2017. Then, he did his postdoctoral research at the Tokyo University of Marine Science and Technology (TUM- SAT). His current research mainly focuses on multi-GNSS precise positioning and GNSS biases analysis.

Bin Wang is currently an associate research scientist of Shanghai Astronomical Observatory (SHAO), Chinese Academy of Sciences (CAS). He received his Ph.D. degree from Wuhan University in 2016. Then, he did his post-doctoral research at the SHAO, CAS. His current research mainly focuses on precise timing and time transfer.